STOICHIOMETRY-DEPENDENT FEAR EFFECT IN A FOOD CHAIN MODEL*

TIANXU WANG† AND HAO WANG‡

Abstract. Evidence shows that resource quality can determine the costs and benefits of fear effect on consumer dynamics. However, mechanistic modeling and analysis are lacking. This paper formulates a tri-trophic level food chain model that integrates both stoichiometric food quality and fear effect. We establish the well-posedness of the model and examine the existence and stability of equilibria. Through extensive numerical simulations, we validate our findings and visually explore the interactive effects of fear and food quality. Our results reveal that the fear effect from predators stabilizes the system. Furthermore, we demonstrate that the fear effect amplifies the influence of food quality on consumers. When food quality is favorable, the fear effect enhances consumer production efficiency, whereas, in the case of poor food quality, the fear effect exacerbates the decline in production efficiency caused by low-nutrient food.

Key words. Producer-consumer-predator, Fear effect, Stoichiometric constraints, Production efficiency, Asymptotic analysis

MSC codes. 92B05, 92D25, 34D05, 34D23, 34C60

1. Introduction.

Prey are influenced by their predators not only by direct killing but also through indirect predation risk [22]. Predation cues generated by predators such as chemical cues can induce fear or alertness in prey [30, 17], subsequently alter the behavior, physiology, and morphology of prey, such as habitat use, foraging behavior, and reproduction rate [16, 61, 50, 19, 15]. This phenomenon is known as the fear effect (also called indirect predation risk or non-consumptive effect). Interestingly, the responses of different species to fear effect vary significantly [38]. Fear effects can be detrimental for some species, causing them to suffer lower mating success, reduced reproductive success, and increased vulnerability to predators [48]. For example, Zanette et al. [68] observed that the perception of predation risk alone led to a 40% decrease in annual offspring production of sparrows. However, fear effects may also positively impact some species by triggering adaptive changes in their life history and behavior. For example, Haapakoski et al. [20] found that exposure to predator cues increased the litter size of voles by 50%, through the effect of alarm pheromones on prey individuals. Similarly, Wen et al. [66] demonstrated that visual and odor cues from predators gave rise to a higher proportion of long-winged female small brown planthoppers which were more agile in evading predation, thereby enhancing their survival rate.

Recent studies have extensively explored the anti-predator response to indirect predation risk. For instance, Leroux et al. [32] employed an ecosystem trophic compartment model to investigate the influence of fear effects on elemental cycling within trophic chains. Wang et al. [65] proposed a two-dimensional predator-prey model in-

*Submitted to the editors DATE.

Funding: The research of Hao Wang was partially supported by the Natural Sciences and Engineering Research Council of Canada (Individual Discovery Grant RGPIN-2020-03911 and Discovery Accelerator Supplement Award RGPAS-2020-00090) and the Canada Research Chairs program (Tier 1 Canada Research Chair Award).

†Department of Mathematical and Statistical Sciences & Interdisciplinary Lab for Mathematical Ecology and Epidemiology, University of Alberta, Edmonton, Alberta T6G 2G1, Canada

‡The Corresponding Author (hao8@ualberta.ca). Department of Mathematical and Statistical Sciences & Interdisciplinary Lab for Mathematical Ecology and Epidemiology, University of Alberta, Edmonton, Alberta T6G 2G1, Canada

corporating the cost of fear into prey reproduction and showed that the anti-predator response stabilized the predator-prey system. Panday et al. [41] extended the study to a tri-trophic food chain model incorporating the cost of fear into reproductions of both prey and middle predator and also demonstrated the stabilizing role of fear. Kaur et al. [29] assumed that zooplankton species had developed defence mechanisms against fish predation and introduced a tri-trophic model, showing that a low level of fear can stabilize the system in the presence of a high rate of zooplankton refuge. Cong et al. [8], Thirthar et al. [59], Ali [1], and Mandal et al. [36] investigated fear effects using three-dimensional food chain models, considering different factors such as reduced production and foraging behavior, harvesting effect of big fish, intra-specific competition among middle predators and top predators, and supplementary food sources, respectively. Their findings consistently indicated that the fear effect contributed to increased stability of the system. Chen et al. [6] considered a modified Leslie–Gower model incorporating fear and Holling type IV functional response with group defence ability of prey. Their study revealed that as the intensity of fear increased, the system underwent multiple dynamic behaviors switching until the final extinction of the prey population. These studies collectively demonstrate that fear effects can lead to complex and diverse population dynamics.

In addition to the fear effect, nutrient availability is another crucial factor for species growth. Ecological stoichiometry is a tool to explore how the balance of energy and multiple chemical elements such as carbon (C), nitrogen (N), and phosphorus (P) affects food-web dynamics and nutrient cycling mechanisms [55]. The proportions of these chemical elements are typically within a certain range to maintain ecosystem stability [18] and meet the nutrient requirement of organisms [26]. These elemental ratios vary across species [11] and even within a single species [47], as different biological processes have diverse nutrient requirements [27]. Variations in elemental ratios can significantly impact the population dynamics [23]. For instance, resources with a higher P:C ratio can be considered as a higher nutrient food, which typically promotes the growth rate and production efficiency of species [57]. Conversely, a lower P:C ratio in prey can constrain the production efficiency of predators, potentially leading to reduced population density and even extinction [34, 10].

The influence of changing the stoichiometric balance on population dynamics has also been widely investigated. For instance, Loladze et al. [34] developed a stoichiometric producer-grazer model (LKE model) and demonstrated that extremely high or low light intensity led to grazer extinction, while moderate light intensity supported the coexistence of three species. Global analyses of the LKE model were conducted by Li et al. [33] and Xie et al. [67]. Moreover, the classical assumptions for LKE model were further studied by [49, 64, 63]. Additionally, several modified models based on the LKE model have been investigated. For example, Wang et al. [62] and Peace et al. [45] explicitly tracked free nutrients in both the prey and the media by spatially homogeneous stoichiometric models. Peace [43] expanded upon the LKE model to a three-dimensional stoichiometric food chain model and predicted that food chain efficiency was reduced when consumers were nutrient-limited. Chen et al. [5] formulated a similar stoichiometric model with maximal production efficiencies of consumers and predators being less than one. Peace and Wang [44] incorporated energetic foraging costs in stoichiometric models and concluded that optimal foraging strategies depend on light and nutrient availability.

Since both fear effects and stoichiometric food quality can significantly influence population dynamics, a natural follow-up question is whether there is an interactive effect between them. In fact, the response of prey to indirect predation risk from

predators is indeed affected by their food [12, 24, 42, 9]. Bell et al. [4] investigated the interaction between fear effects and food quality (measured as P:C) in an experimental setting involving a food chain of algae, daphnia, and fish. They found that the reduction in survival rates and population growth rates that resulted from low-nutrient food were amplified in the presence of predator-derived cues. Conversely, when the food quality was good, these chemical cues led to a higher population growth rate. A potential reason is that daphnia typically responds to predator-derived chemical cues by reproducing earlier and at a smaller size [56], which requires higher resource investments for initial reproduction [69]. Poor food quality thus constrains the reproduction rate and growth rate of daphnia, while high-nutrient food may enhance its reproduction rate, ultimately resulting in an increasing population.

Although the influence of fear effect on population dynamics is highly dependent on food quality, most (if not all) existing predator-prey models neglect the interactive effect of fear effect and food quality. This paper aims to address this limitation by proposing a three-dimensional food chain model that integrates both indirect predation risk and stoichiometric constraints. Through rigorous analysis, we try to gain a deeper understanding of how these two factors interactively shape population dynamics.

The remainder of this paper is organized as follows. In section 2, we provide the mathematical model. In section 3, we present a preliminary mathematical analysis of the model. In section 4, extensive numerical simulations are given to further prove the analysis and delineate some interesting findings. In section 5, we provide a summary of the results.

2. Model formulation. This study focuses on the interaction among producers, consumers, and predators in a closed ecological system. The food chain of algae, daphnia, and fish can be viewed as a special case. We follow a coarse outline in [5]. Recall the general form of a basic three-dimensional food chain model, similar to the model described in [21]:

$$\begin{cases} \dfrac{\mathrm{d}x}{\mathrm{d}t} = bx\left(1-\dfrac{x}{K}\right) - f(x)y, \\ \dfrac{\mathrm{d}y}{\mathrm{d}t} = e_y f(x)y - g(y)z - d_y y, \\ \dfrac{\mathrm{d}z}{\mathrm{d}t} = e_z g(y)z - d_z z, \end{cases} \tag{2.1}$$

where $x(t)$, $y(t)$, and $z(t)$ represent the density of producers, consumers, and predators respectively. The functions $f(x)$ and $g(y)$ are consumer and predator ingestion rates, respectively. In general, $f(x)$ and $g(y)$ are bounded differentiable and satisfy $f(0) = 0$, $f'(x) > 0$, $f''(x) < 0$ for $x \geq 0$; $g(0) = 0$, $g'(y) > 0$, $g''(y) < 0$ for $y \geq 0$. Furthermore, $f(x)$ and $g(y)$ are saturating with $\lim\limits_{x\to\infty} f(x) = \hat{f}$ and $\lim\limits_{y\to\infty} g(y) = \hat{g}$, respectively. In our study, we take $f(x)$ and $g(y)$ as Holling type II functional responses, i.e., $f(x) = \frac{c_1 x}{a_1+x}$ and $g(y) = \frac{c_2 y}{a_2+y}$, where a_1, a_2, c_1, and c_2 are explained in Table 1. The remaining parameters are provided in Table 1.

This classic food chain model assumes that producers are always provided with ample nutrients and their growth is only limited by light intensity. However, in real ecosystems, limited resources and nutrients are more common. Therefore, incorporating stoichiometric constraints into the model is needed. We express biomass in terms of C since C makes up the bulk of the dry weight of most organisms. P is often a limiting nutrient in aquatic systems [13] and all organisms require a certain

species-specific fraction of P for survival. Hence, we consider two essential elements: C and P. Note that one can also choose other essential parameters (e.g., nitrogen, sulfur, or calcium) [34]. In this study, the P:C ratio will be used to assess nutrient levels.

On the other hand, traditional fear effect models always assume that the fear effect decreases the growth rate of consumer population. However, the response of prey to fear effect has been observed to be dependent on food quality [4]. Moreover, as the density of predators increases, the prey species typically exhibit more robust fear responses, indicating that the fear effect becomes more pronounced with higher predator densities.

In this study, we make the following assumptions:

(A1) The total amount of phosphorus in the ecosystem is constant, denoted by P (mgP/l).

(A2) The P:C ratio of producers varies, but never falls below a minimum value of Q_m (mgP/mgC). Consumers and predators maintain constant P:C ratios, denoted by θ_y and θ_z (mgP/mgC), respectively.

(A3) All phosphorus in the system is divided into three pools: producers, consumers, and predators. The phosphorus in producers must remain above a certain minimum level, denoted by P_m (mgP/l).

(A4) As the predator density increases, the impact of fear becomes more pronounced.

The population densities are measured in terms of carbon. From assumptions (A1), (A2), and (A3), P available for the producer is $P-\theta_y y-\theta_z z$ (mgP/l). Therefore, the producer's P:C ratio can be represented as

$$Q = \frac{P - \theta_y y - \theta_z z}{x} \tag{2.2}$$

(mgP/mgC). Furthermore, by assumption (A2), P:C in producers has a minimum value Q_m, an upper bound for producer density thus can be expressed as $\frac{P-\theta_y y-\theta_z z}{Q_m}$ (mgC/l). Additionally, producer density can not exceed K (mgC/l) due to light intensity availability. Therefore, the combination of external factor (light intensity) and internal factor (P availability) limits the carrying capacity of the producer to $\min\left\{K, \frac{P-\theta_y y-\theta_z z}{Q_m}\right\}$.

Next, we show how stoichiometric food quality affects the production efficiency of consumers. Q indicates the nutrient level of producers. When Q is greater than or equal to the P:C ratio required by consumers (i.e., $Q \geq \theta_y$), the food quality for consumers is optimal. In this scenario, consumers are able to maximize their utilization of energy (carbon). However, a lower P:C ratio in producers (i.e., $Q < \theta_y$) indicates lower nutrient food quality for consumers, resulting in limited production efficiency. The limitation of food quality to the production efficiency of consumers thus can be represented as a minimum function, $\min\left\{1, \frac{Q}{\theta_y}\right\}$. Similarly, the production efficiency of predators is also limited by their food quality, which can be represented by $\min\left\{1, \frac{\theta_y}{\theta_z}\right\}$.

Furthermore, we investigate impact of fear effect induced by predators on consumer production efficiency. The magnitude of fear effect is strongly influenced by food quality [4] and population density of predators (assumption (A4)). As the nutrient level of producers falls below optimal conditions, the production efficiency of consumer population becomes constrained. However, the presence of fear effect further

Table 1: The parameters for system (2.1) and (2.4).

Para.	Description	Value	Unit	Source
P	total phosphorus	0.12	mgC/l	[5]
e_y	maximal production efficiency of consumers	0.95	no unit	Assumed
h_m	minimal production efficiency of consumers	0.4	no unit	Assumed
$\bar{e}_y$	threshold for maximal production efficiency in consumers	0.7	no unit	Assumed
e_z	maximal production efficiency of predators	0.75	no unit	[5]
b	maximum growth rate of producers	1.2	day^{-1}	[5]
d_y	consumer loss rate (include respiration)	0.25	day^{-1}	[5]
d_z	predator loss rate (include respiration and predation)	0.003	day^{-1}	[5]
θ_y	consumer constant P : C	0.03	mgP/mgC	[5]
θ_z	predator constant P : C	0.013	mgP/mgC	[5]
Q_m	minimal P:C in producers	0.0008	mgP/mgC	[31]
$\bar{Q}$	threshold value of P:C in producers	0.00079-0.09	mgP/mgC	[4, 14, 31]
c_1	maximal ingestion rate of the consumer	0.81	day^{-1}	[5]
c_2	maximal ingestion rate of the predator	0.03	day^{-1}	[5]
a_1	half-saturation of the consumer ingestion response	0.25	mgC/l	[5]
a_2	half-saturation of the predator ingestion response	0.75	mgC/l	[5]
K	producer carrying capacity limited by light	0-10	mgC/l	[5]
ρ	fear effect coefficient	0-4	no unit	Assumed
β	half-saturation constant of fear effect response	56	mgC/l	Assumed
γ	half-saturation constant for food quality	0.01	mgP/mgC	Assumed

Notes: Most parameters correlated with producers (e.g., phytoplankton) and consumers (e.g., zooplankton) are selected from [2, 60] and are used in [5, 46, 34, 43]. The parameters correlated with predators (e.g., fish) are chosen from [28, 35] and are used in [5]. For the P:C ratio in producers, the ranges recorded in [4, 14, 31] are 0.0016-0.01, 0.04-0.09, and 0.00079-0.0295, respectively. Therefore, in this paper, we consider the range of $\bar{Q}$ to be 0.00079-0.09. In particular, we use $\bar{Q} = 0.03$ and 0.0033 in simulations. To capture more dynamics, we choose the minimal P:C ratio Q_m relatively low at 0.0008. The maximal production efficiency of consumers e_y is usually assumed to be higher than 0.8 in [2, 34, 46, 43, 5]; here, it is assumed to be 0.95. The minimal production efficiency of consumers h_m is chosen as 0.4. The threshold $\bar{e}_y$ between e_y and h_m is assumed to be 0.7.

exacerbates this reduction. On the other hand, when the nutrient level of producers is optimal, there are no limitations imposed by food quality, and fear effect from predators can potentially enhance the production efficiency of consumer population.

Let $\bar{Q}$ denote the threshold value of the P:C ratio in producers. We summarize the above analysis as the following conclusions:

1. As producer P:C ratio increases within a specific range, consumer production efficiency also increases. However, beyond this range, further increases in P:C ratio do not affect consumer production efficiency.

2. When producer P:C ratio is higher than $\bar{Q}$, fear effect enhances consumer production efficiency.

3. When producer P:C ratio is higher than $\bar{Q}$, increasing predator density intensifies the positive effect of fear on consumer production efficiency.

4. When producer P:C ratio is lower than $\bar{Q}$, fear effect reduces consumer production efficiency.

5. When producer P:C ratio is lower than $\bar{Q}$, increasing predator density intensifies the negative effect of fear on consumer production efficiency.

6. When producer P:C ratio is equal to $\bar{Q}$, fear effect does not influence consumer production efficiency.

We now introduce the function $h(z, Q)$ to capture the varying production efficiency due to fear effect as follows:

$$h(z,Q) = \rho\frac{\alpha(Q)z}{z+\beta} + \bar{e}_y, \qquad \alpha(Q) = \frac{Q-\bar{Q}}{Q+\gamma}, \tag{2.3}$$

where $\bar{e}_y$ is a threshold value, representing the maximal production efficiency of consumers in the absence of fear effect or when fear effect does not influence consumer growth. Q is given in (2.2). Parameters ρ, β, and γ can be found in Table 1. Figure 1 visually depicts the function $h(z, Q)$. Figure 1a shows $h(z, Q)$ in terms of z while keeping Q fixed, and Figure 1b shows $h(z, Q)$ in terms of Q while keeping z fixed. The system (2.4) eventually reaches a stable equilibrium, periodic state, or chaotic state, without diverging to infinity. As a result, Figure 1a demonstrates distinct finite ranges for z in each of the three cases.

The function $h(z, Q)$ satisfies following properties, which align with the above conclusions:

1. $h(z, Q)$ is an increasing function with respect to Q up to a certain point, after which it remains constant, as shown in Figure 1b.
2. As $Q > \bar{Q}$, $\bar{e}_y < h(z, Q) < e_y < 1$, as shown in Figure 1a.
3. As $Q > \bar{Q}$, $h(z, Q)$ is an increasing function over z, as shown in Figure 1a.
4. As $Q < \bar{Q}$, $0 < h_m < h(z, Q) < \bar{e}_y$, where h_m denotes the minimum value of $h(z, Q)$, as shown in Figure 1a.
5. As $Q < \bar{Q}$, $h(z, Q)$ is a decreasing function over z, as shown in Figure 1a.
6. As $Q = \bar{Q}$, $\alpha(Q) = 0$, $h(z, Q) = \bar{e}_y$, as shown in Figure 1a.

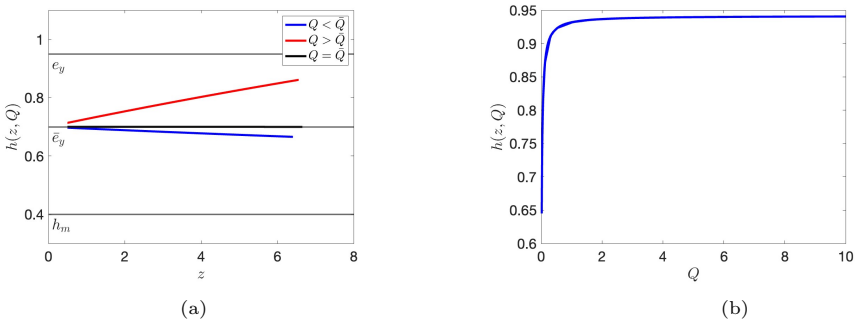

(a) (b)

Fig. 1: Function $h(z, Q)$. (a) When $Q > \bar{Q}$, $h(z, Q)$ is an increasing function of z. When $Q < \bar{Q}$, $h(z, Q)$ is a decreasing function of z. When $Q = \bar{Q}$, $h(z, Q) = \bar{e_y}$. We set $\bar{Q} = 0.03$ for $Q > \bar{Q}$, $\bar{Q} = 0.0033$ for $Q < \bar{Q}$, and $\bar{Q} = 0.024$ for $Q = \bar{Q}$. The value of ρ is set to 2.5. (b) $h(z, Q)$ is an increasing function of Q. We set $\bar{Q} = 0.03$. The initial values are $(x(0), y(0), z(0)) = (0.5, 0.5, 0.5)$ and other parameters are listed in Table 1.

Based on above analysis, we obtain a new food chain model incorporating both

stoichiometric food quality and fear effect as follows:

(2.4)
$$\begin{cases} \dfrac{\mathrm{d}x}{\mathrm{d}t} = \underbrace{bx\left(1-\dfrac{x}{\min\left\{K,\frac{P-\theta_y y-\theta_z z}{Q_m}\right\}}\right)}_{\text{growth limited by light and nutrient}} - \underbrace{f(x)y}_{\text{consumed by consumers}}, \\ \dfrac{\mathrm{d}y}{\mathrm{d}t} = \underbrace{h(z,Q)\min\left\{1,\dfrac{Q}{\theta_y}\right\}f(x)y}_{\text{growth limited by fear effect, food quality and quantity}} - \underbrace{g(y)z}_{\text{consumed by predators}} - \underbrace{d_y y}_{\text{death}}, \\ \dfrac{\mathrm{d}z}{\mathrm{d}t} = \underbrace{e_z\min\left\{1,\dfrac{\theta_y}{\theta_z}\right\}g(y)z}_{\text{growth limited by food quality and quantity}} - \underbrace{d_z z}_{\text{death}}, \end{cases}$$

where Q and $h(z,Q)$ are given by (2.2) and (2.3), respectively.

3. Qualitative analysis.

3.1. Positivity and boundedness. The following theorems show that system (2.4) is biologically well defined. The proofs for these theorems can be found in Appendix A. First, we verify the biological validity of the model when x approaches zero.

THEOREM 3.1. *The model* (2.4) *is well defined as* $x \to 0$.

This theorem confirms that as x approaches zero, the system does not undergo any explosions or catastrophic failures. Next, we find a bounded positive set that all solutions of the system (2.4) eventually enter. Let

$$\Omega = \{(x,y,z):\ 0 \le x \le k,\ 0 \le y \le P/\theta_y,\ 0 \le z \le P/\theta_z,\ Q_m x + \theta_y y + \theta_z z \le P\},$$

where $k = \min\left\{K, \frac{P}{Q_m}\right\}$. The region Ω is a closed triangular truncated cone (if $K < \frac{P}{Q_m}$) or a closed triangular pyramid (if $K \ge \frac{P}{Q_m}$). It is separated into two parts by the plane $\theta_y x + \theta_y y + \theta_z z = P$. The inner region is denoted as region I, and the outer region is denoted as region II, as illustrated in Figure 2. The following theorem shows that solutions with an initial state in the set Ω will remain in Ω for all forward time.

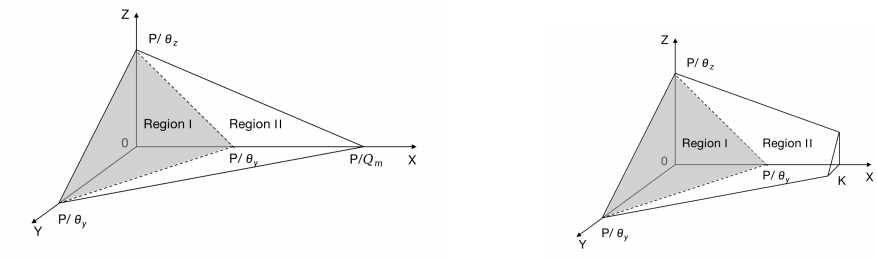

Fig. 2: The positively invariant set Ω. (a) As $K \ge \frac{P}{Q_m}$, Ω is a triangular pyramid. (b) As $K < \frac{P}{Q_m}$, Ω is a triangular truncated cone. The plane $\theta_y x + \theta_y y + \theta_z z = P$ separates Ω into two regions.

THEOREM 3.2. *Ω is positively invariant for semiflow generated by system* (2.4).

Therefore, if the initial population densities of three species are non-negative, they will remain non-negative throughout, regardless of varying environmental conditions and disturbances.

3.2. Equilibria analysis. We further explore the long-term behavior of model (2.4) by examining the system's equilibria. The possible equilibria consist of the boundary equilibria $E_0(0,0,0)$, $E_1(k,0,0)$, and $E_2(\bar{x},\bar{y},0)$, as well as internal equilibria $E^*(x^*,y^*,z^*)$. Detailed mathematical analysis and proofs can be found in Appendix B.

We begin with the stability analysis of the extinction equilibrium $E_0(0,0,0)$.

THEOREM 3.3. *The extinction equilibrium $E_0(0,0,0)$ is unstable.*

Biologically, this implies that this ecosystem will never collapse completely. Next, we analyze the stability of the producer-only equilibrium $E_1(k,0,0)$.

THEOREM 3.4. *The producer-only equilibrium $E_1(k,0,0)$ is locally asymptotically stable (LAS) if $\bar{e}_y \min\left\{1, \frac{P}{k\theta_y}\right\} f(k) < d_y$.*

Therefore, when the death rate of consumers exceeds their growth rate, both consumers and predators will die out, leaving only producers to survive. The population density of producers will eventually stabilize at the maximum carrying capacity limited by the availability of light and phosphorus, i.e., $k = \min\left\{K, \frac{P}{Q_m}\right\}$.

The existence of the producer-consumer equilibrium $E_2(\bar{x},\bar{y},0)$ depends on the growth and death rates of consumers. To ensure the survival of consumers, the growth rate of consumers must be greater than their death rate. Conversely, the death rate of predators should exceed their growth rate, leading to their eventual extinction. These conditions can be captured by the following inequalities:

$$G(k,0,0) = \bar{e}_y \min\left\{1, \frac{P}{\theta_y}\right\} f(x) - d_y > 0, \tag{3.1}$$

$$H(\bar{x},\bar{y}_{\max},0) = e_z \min\left\{1, \frac{\theta_y}{\theta_z}\right\} g(\bar{y}_{\max}) - d_z < 0, \tag{3.2}$$

where $\bar{y} \le \bar{y}_{\max} = \frac{P}{\theta_y} - f^{-1}\left(\frac{d_y}{\bar{e}_y}\right)$, as discussed in Appendix B.3. Inequalities (3.1) and (3.2) provide sufficient conditions for the existence of E_2.

The stability of equilibrium E_2 can be determined by analyzing the nullclines of the producer and consumer.

THEOREM 3.5. *In region I ($x + y < \frac{P}{\theta_y}$), E_2 is LAS if the producer nullcline is decreasing, and E_2 is unstable if it is increasing. In region II ($x + y > \frac{P}{\theta_y}$), E_2 is LAS if the slope of the consumer nullcline is higher than the slope of the producer nullcline; otherwise, E_2 is unstable.*

Biologically, this implies that when the producer's growth rate is much faster than that of grazers, eventually, producers, grazers, and predators can all survive. If the producer's growth rate is positive but their increasing speed is not very rapid, then grazers can survive, but predators cannot survive.

For the coexistence equilibrium $E^*(x^*, y^*, z^*)$, define

$$L_1 := \frac{e_y x^* c_1}{a_1} - d_y - \frac{c_2 z^*}{a_2 + P/\theta_y},$$

$$L_2 := \frac{e_z \min\left\{1, \frac{\theta_y}{\theta_z}\right\} y^* c_2}{a_2} - d_z,$$

$$L_3 := d_y e_z \min\left\{1, \frac{\theta_y}{\theta_z}\right\} y^* + d_z z^* - e_y e_z \min\left\{1, \frac{\theta_y}{\theta_z}\right\} b x^*,$$

$$L_4 := e_z \min\left\{1, \frac{\theta_y}{\theta_z}\right\} \left[\left(\frac{k}{\min\left\{K, \frac{P_m}{Q_m}\right\}} - 1 \right) e_y b x^* + (d_y \right.$$

$$\left. - h_m \min\left\{1, \frac{Q_m}{\theta_y}\right\} \frac{a_1}{c_1 + k} k \right) y^* + \left(1 - \frac{k}{K}\right) e_y b k \Bigg] + d_z z^*,$$

then the following theorem provides a sufficient condition for the global stability of the internal equilibrium $E^*(x^*, y^*, z^*)$.

THEOREM 3.6. *The internal equilibrium $E^*(x^*, y^*, z^*)$ is globally asymptotically stable (GAS) if $L_i \leq 0$ for i=1,2,3,4 and at least one of these inequalities is strictly negative.*

In subsection 4.1, we provide a numerical example to further illustrate the practical application of this theorem.

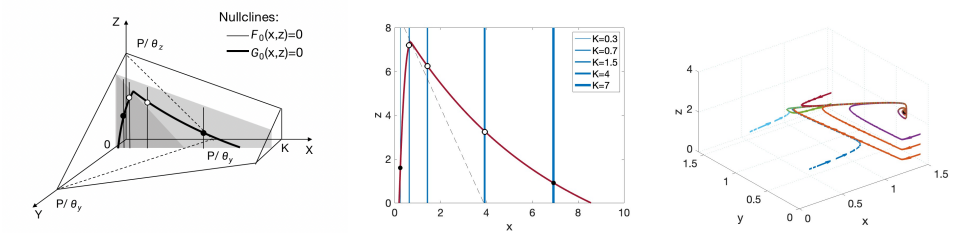

(a) (b) (c)

Fig. 3: (a) Stoichiometry confined feasible region Ω in phase space. The shaded surface is defined by $y = y^*$. (b) Internal equilibrium in x-z plane as $y = y^*$. The blue curves refer to $F_0(x, z)$ for different K values, and the peak-shaped curve is defined by $G_0(x, z)$. The intersection points of $F_0(x, z)$ and $G_0(x, z)$ are internal equilibria. The solid dot implies the stable equilibrium while the circle denotes the unstable equilibrium. (c) E^* is GAS.

4. Numerical simulation. In this section, we study the system (2.4) with the help of numerical simulation. The parameters are shown in Table 1. We set the initial state as $(x(0), y(0), z(0)) = (0.5, 0.5, 0.5)$ for all simulations.

4.1. Numerical analysis of internal equilibria. If the system (2.4) admits an internal equilibrium $E^*(x^*, y^*, z^*)$, we can solve y^* from $H(x^*, y^*, z^*) = 0$:

$$y^* = g^{-1}\left(\frac{d_z}{e_z \min\left\{1, \frac{\theta_y}{\theta_z}\right\}} \right).$$

Therefore, we can degenerate the system into a two-dimensional x-z system by fixing $y = y^*$. This allows us to study the internal equilibrium of the system (2.4) on the x-z plane, as depicted in Figure 3a. For convenience, we denote $F(x, y^*, z)$ and $G(x, y^*, z)$ as $F_0(x, z)$ and $G_0(x, z)$, respectively. Intersections of $F_0(x, z)$ and $G_0(x, z)$ represent internal equilibria. Figure 3b illustrates that there exists at most one internal equilibrium in all cases.

We provide an example to demonstrate the application of Theorem 3.6 using the following parameter values: $b = 0.8$, $d_y = 0.005$, $d_z = 0.0003$, $a_1 = 8$, $a_2 = 2$, $P = 0.06$, $K = 1.25$, $\rho = 4$, $e_y = 0.2$, $P_m = 0.001$, and $h_m = 0.4$. The remaining parameters are specified in Table 1. With these parameter values, we obtain $L_1 = -0.0019 < 0$, $L_2 = 0$, $L_3 = -0.0001 < 0$, and $L_4 = -0.1486 < 0$, which satisfy all the conditions stated in Theorem 3.6. Therefore, we can conclude that the equilibrium point $E^* = (1.2465, 0.0269, 2.9515)$ is GAS, which is further supported by the simulation results shown in Figure 3c.

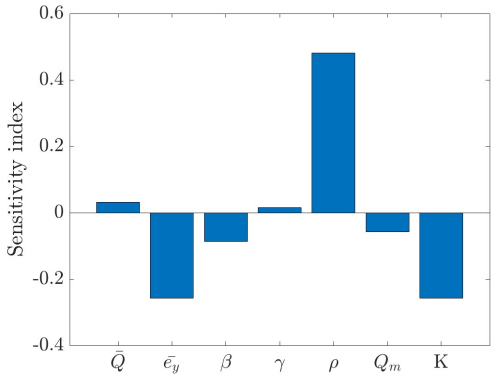

Fig. 4: Sensitivity analysis for Q, $\bar{e_y}$, β, γ, ρ, Q_m and K.

4.2. Sensitivity analysis. We perform the sensitivity analysis by calculating the partial ranked correlation coefficient (PRCC) with respect to the consumer population to assess the influence of different parameters as shown in Figure 4. The threshold value for maximal production efficiency of consumers, $\bar{e}_y$, exhibits a relatively high sensitivity index. From equation (2.3), it is obvious that $\bar{e}_y$ directly influences the production efficiency of consumers. In this paper, we chose a reasonable value of 0.7 for $\bar{e}_y$. Another parameter that demonstrates notable sensitivity is K, which represents light intensity input into the system. Light intensity indirectly influences the quality and quantity of food available to consumers. Moreover, the fear effect coefficient (i.e., ρ), indicating the magnitude of the fear effect, exhibits the highest sensitivity. This suggests that even slight changes in fear effect can have a substantial impact on the system dynamics. We will further investigate the roles of these two parameters, K and ρ, in the following sections.

4.3. Influence of light intensity. Light intensity plays a crucial role in the carbon synthesis of producers, subsequently affecting their nutrient levels. Inadequate light intensity has been shown to result in reduced carbon assimilation [58]. Conversely, strong light intensity often leads to abundant carbon, which results in a low P:C ratio in producers. In this section, we choose K as a bifurcation parameter

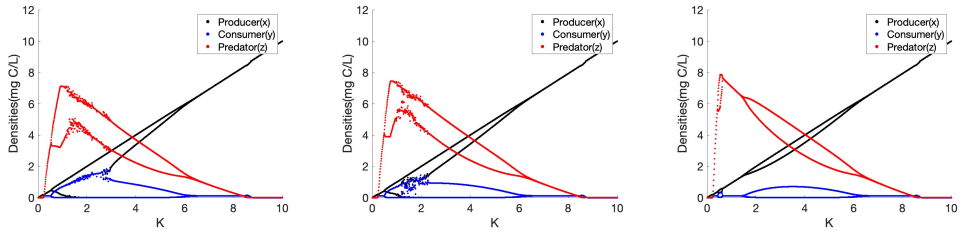

(a) $\rho = 0$ (b) $\rho = 1$ (c) $\rho = 2.7$

Fig. 5: Bifurcation diagrams over K. (a) ρ=0. (b) ρ=1. (c) ρ=2.7.

to investigate how light intensity influences the system, as shown in Figure 5. Additionally, Figure 6 presents the time series of the system (2.4). Figure 7 illustrates the corresponding trajectories in three-dimensional phase space.

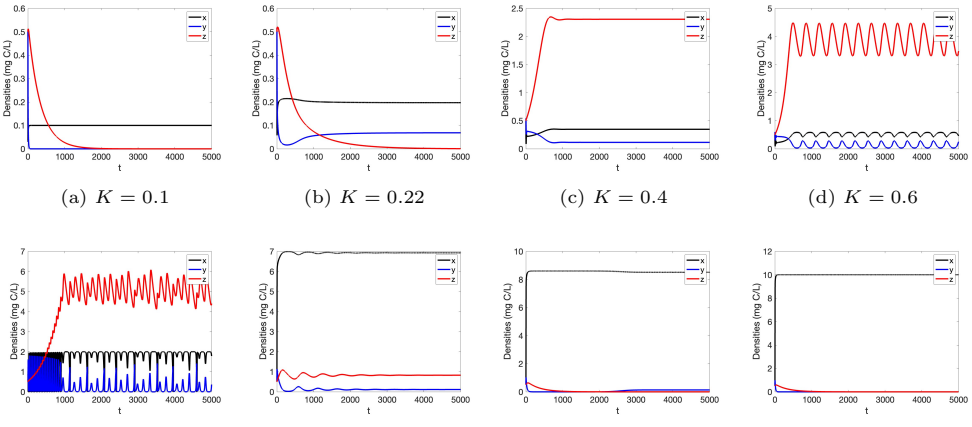

(a) $K = 0.1$ (b) $K = 0.22$ (c) $K = 0.4$ (d) $K = 0.6$

(e) $K = 2$ (f) $K = 7$ (g) $K = 8.6$ (h) $K = 10$

Fig. 6: Time series of the system (2.4) without fear effect. (a) $K = 0.1$, producer-only equilibrium E_1 is stable. (b) $K = 0.22$, producer-consumer equilibrium E_2 is stable. (c) $K = 0.4$, coexistence equilibrium E^* is stable. (d) $K = 0.6$, system (2.4) admits a limit circle. (e) $K = 2$, system (2.4) is chaotic. (f) $K = 7$, coexistence equilibrium E^* is stable. (g) $K = 8.6$, producer-consumer equilibrium E_2 is stable. (h) $K = 10$, producer-only equilibrium E_1 is stable. We take $\bar{Q}$=0.0033. Other parameters are specified in Table 1.

We first discuss the case when there is no fear effect. i.e., ρ=0 (Figure 5a). Extremely low light intensity ($0 < K < 0.2$) can only support the survival of producers at very low densities. However, both consumers and predators go extinct due to the lack of food, as depicted in Figure 5a. A specific scenario for $K = 0.1$ is shown in Figure 6a. When the light intensity is increasing but still at a relatively low level ($0.2 < K < 0.23$), both producers and consumers can coexist, and the boundary equilibrium E_2 is stable (e.g., $K = 0.22$ in Figure 6b and Figure 7b). As light intensity increases further, it becomes sufficient to support the survival of the entire system. In the range of $0.23 \leq K \leq 0.52$, a unique stable internal equilibrium emerges, indicating that all three species coexist in a stable state (e.g., $K = 0.4$ in Figure 6c

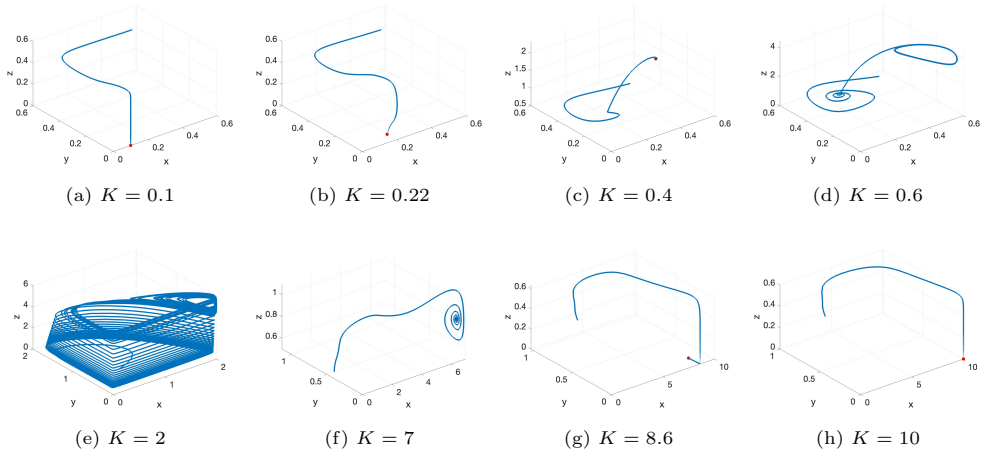

(a) $K = 0.1$ (b) $K = 0.22$ (c) $K = 0.4$ (d) $K = 0.6$

(e) $K = 2$ (f) $K = 7$ (g) $K = 8.6$ (h) $K = 10$

Fig. 7: Trajectories of the system (2.4) in phase space without fear effect. (a) $K = 0.1$, producer-only equilibrium E_1 is stable. (b) $K = 0.22$, producer-consumer equilibrium E_2 is stable. (c) $K = 0.4$, coexistence equilibrium E^* is stable. (d) $K = 0.6$, system (2.4) admits a limit circle. (e) $K = 2$, system (2.4) is chaotic. (f) $K = 7$, coexistence equilibrium E^* is stable. (g) $K = 8.6$, producer-consumer equilibrium E_2 is stable. (h) $K = 10$, producer-only equilibrium E_1 is stable. We take $\bar{Q}$=0.0033. Other parameters are specified in Table 1.

and Figure 7c).

When light intensity reaches an intermediate threshold value ($K = 0.52$), a Hopf bifurcation occurs, resulting in abrupt changes in the dynamics of the system (2.4). As light intensity continues to increase ($0.52 < K < 1.1$), the densities of three species exhibit periodic variations. Figure 6d and Figure 7d illustrate the presence of a limit cycle when $K = 0.6$. However, as K surpasses 1.1, the system undergoes a transition to chaotic dynamics (e.g., $K = 2$ in Figure 6e and Figure 7e). As light intensity further increases ($3 \leq K \leq 6.5$), the system transitions back to a limit cycle with the amplitude of the limit cycle gradually decreasing to zero. At $K = 6.5$, another Hopf bifurcation occurs. With even higher light intensities ($6.5 < K < 8.54$), the system converges to a stable internal equilibrium again (e.g., $K = 7$ in Figure 6f and Figure 7f).

Note that as light intensity increases, producers are able to synthesize more carbon, leading to a decrease in their P:C ratio. As a result, the densities of consumers and predators tend to decrease as their primary food source becomes less nutritious. When the light intensity is large ($8.54 < K < 8.73$), food quality for consumers is too low to sustain the survival of predators. (e.g., $K = 8.6$ in Figure 6g and Figure 7g). Further increasing light intensity ($K > 8.73$), extremely low nutrient food causes consumers to perish as well (e.g., $K = 10$ in Figure 6h and Figure 7h).

4.4. Fear effect stabilizes the system. In a predator-prey system, the fear effect can significantly impact the behavior of prey, including their habitat use, foraging behavior, metabolic rate, and reproduction rate [16, 61, 19]. In this section, we investigate the role of fear effect through bifurcation diagrams.

We discussed the case when there is no fear effect in subsection 4.3. However, as the magnitude of the fear effect increases, the previously observed chaos interval gradually fades out, leading to a more stable system, as illustrated in Figure 5. Under the

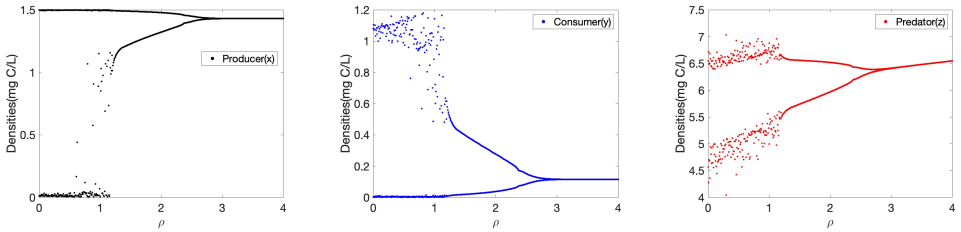

(a) Producer (b) Grazer (c) Predator

Fig. 8: Bifurcation diagram over fear effect coefficient ρ.

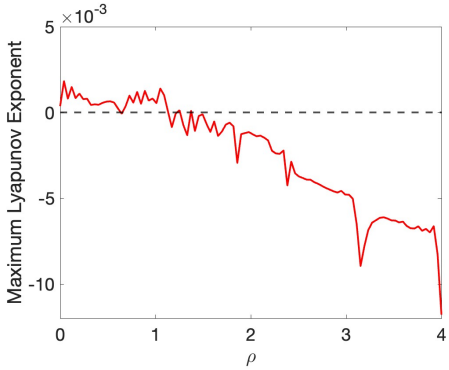

Fig. 9: The maximum Lyapunov exponent with respect to the fear effect coefficient ρ.

presence of strong fear effects, the influence of light intensity on population dynamics can be significantly different. For instance, when $\rho = 2.7$, chaos is no longer observed as light intensity increases. Instead, a distinct pattern emerges, characterized by a periodic oscillation followed by a stable state, and then another periodic oscillation. This shift in behavior highlights the stabilizing effect of fear on the system.

The parameter ρ represents the magnitude of the fear effect. We further explore the influence of the fear effect through bifurcation diagrams across varying values of ρ, as shown in Figure 8. We set $K = 1.5$, $\bar{Q} = 0.0033$, and keep the remaining parameters as specified in Table 1. When the fear effect is weak ($\rho < 1.2$), the system exhibits chaotic behavior. This is also evidenced by Figure 9, where the maximum Lyapunov exponent is positive. As the fear effect increases ($1.2 < \rho < 2.9$), the system displays periodic dynamics with the amplitude of the limit cycle gradually decreasing to zero. This correlation is supported by Figure 9, where the maximum Lyapunov exponent is negative, indicating the absence of chaos and a growing stability in the system. Further increasing fear effect ($\rho > 2.9$) leads the system to converge towards a unique stable equilibrium. These results further suggest that stronger fear effects promote system stability.

4.5. Strong fear effect promotes trophic energy transfer efficiency. Beyond stability, the influence of the fear effect varies significantly among different trophic populations. Figure 10 illustrates the mean population densities affected by the fear effect. When the fear effect is relatively weak, the mean population density

of grazers decreases, while both producers and predators exhibit the opposite trend. However, as the fear effect strengthens further, the populations of producers and grazers stabilize at a constant level, while the predator population continues to rise. This suggests that a low fear effect promotes producer growth, and predators consistently benefit from the fear effect, even at higher levels.

Given the substantial variation in the effect of fear on different trophic populations, we also aim to determine the trophic energy transfer efficiency. The trophic energy transfer efficiencies between producers and grazers, and between grazers and predators, are defined as follows:

$$R_1 = h(z, Q)\min\Big\{1, \frac{Q}{\theta_y}\Big\}, \tag{4.1}$$

$$R_2 = e_z \min\Big\{1, \frac{\theta_y}{\theta_z}\Big\}. \tag{4.2}$$

The trophic transfer efficiency between producers and predators is then given by $R_1 R_2$. The mean trophic energy transfer efficiency is illustrated in Figure 10d. When the fear effect is in a low range, the influence of fear effect to trophic transfer effciciency is not obvious. However, when the fear effect is relatively strong, as ρ increases, the mean trophic efficiency shows an increasing trend. This also aligns with the variation in population density.

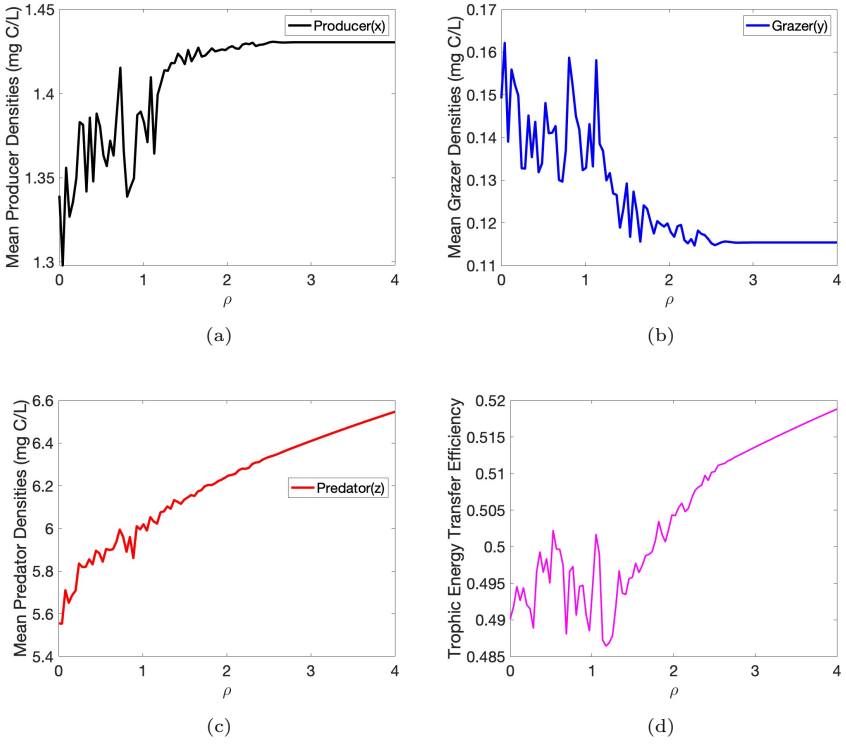

Fig. 10: Impact of fear effect on mean population density across trophic levels: (a) Producer, (b) Grazer, (c) Predator, and on (d) Mean trophic energy transfer efficiency.

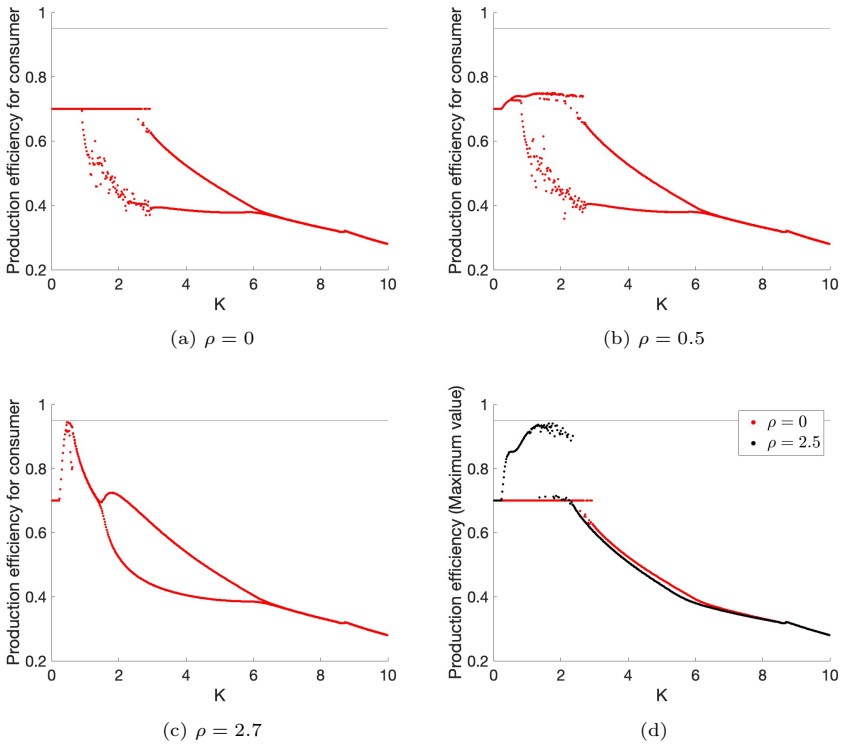

Fig. 11: (a) Production efficiency for consumers as ρ=0. (b) Production efficiency for consumers as ρ=0.5. (c) Production efficiency for consumers as ρ=2.7. (d) The maximum value of Production efficiency for consumers as ρ=2.5, compared with the case ρ=0.

4.6. Fear effect amplifies the impact of food quality. The production efficiency of consumers is given by R_1 in (4.1). In this section, we aim to investigate the interactive effect of fear effect and food nutrients on consumer production efficiency. We consider two cases with different threshold values of nutrient level in producers (i.e., $\bar{Q}$).

In the first case, we consider a relatively low threshold value, $\bar{Q} = 0.0033$. In this scenario, the P:C ratio in producers (i.e., Q) always remains higher than $\bar{Q}$.

When there is no fear effect present (i.e., $\rho = 0$), the production efficiency solely depends on the food nutrient level, which is influenced by light intensity. When the light intensity is relatively low ($K < 0.23$), the high P:C ratio in producers does not restrict consumer growth. As a result, the production efficiency for consumers remains constant ($\bar{e}_y$), as shown in Figure 11a. As light intensity increases, producers are capable of synthesizing more carbon, leading to a decrease in the intrinsic P:C ratio. When the P:C ratio of producers falls below the consumer's P:C ratio θ_y, consumers are unable to fully utilize all the nutrients available in the producers. As a result, the production efficiency of consumers starts to decline, as depicted in Figure 11a.

Next, we introduce the fear effect into the system. Under extremely low light intensity ($K < 0.23$), predators cannot survive due to scarcity of food. Consequently, there is no fear effect exerted by predators, and the production efficiency for consumers

remains constant ($\bar{e}_y$). As light intensity reaches a level that can sustain the survival of all three species ($0.23 < K < 8.54$), the fear effect starts to influence the production efficiency of consumers. When the light intensity is in a moderate range where the nutrient level of producers is optimal for consumers, the presence of indirect predation risk from predators enhances the production efficiency of consumers, as shown in Figure 11b and Figure 11c. This implies that when $Q > \bar{Q}$, the fear effect can amplify the positive impact of high food quality on the growth of consumers. Moreover, stronger fear effects result in a more pronounced increase in production efficiency.

We now consider the second case where the threshold of food nutrients is relatively high ($\bar{Q} = 0.03$). Figure 11d compares the maximum value of production efficiency for consumers between $\rho = 2.5$ and $\rho = 0$. In the case of extremely low light intensity ($K < 0.23$) or extremely high light intensity ($K > 8.7$), there is no fear effect generated by predators, as predators cannot survive due to limited quantity or low-quality food (see the discussion in subsection 4.3). Therefore, the curves of the maximum value of production efficiency for $\rho = 2.5$ and $\rho = 0$ collapse into a single curve. When the light intensity is in a moderate range ($0.23 < K < 2.26$), the nutrient level in producers is relatively high and exceeds $\bar{Q}$ (i.e., $Q > \bar{Q}$). In this case, the presence of the fear effect significantly promotes the maximal production efficiency of consumers, as shown in Figure 11d. On the other hand, when light intensity is high ($2.26 < K < 8.7$), nutrient level in producers is relatively low and falls below $\bar{Q}$ (i.e., $Q < \bar{Q}$). In this case, the production efficiency decreases as light intensity increases, and the presence of the fear effect further exacerbates this decline. This implies that fear effect can amplify the impact of food quality on the growth of consumers.

5. Discussion. The response of prey to fear effect has been observed to be dependent on food quality in a recent experimental study [4]. However, previous studies treated fear effects and food quality as separate factors without establishing a connection between them. To bridge this gap, we proposed a novel three-dimensional food chain model (2.4) that integrates stoichiometric food quality and fear effects. Notably, food quality for consumers can be indirectly influenced by light intensity. Therefore, in this study, we conducted a rigorous analysis to explore the influence of light intensity, fear effect, and the interactive effect of food quality and fear effect on population dynamics.

Mathematical analysis reveals that our system is resilient and will never go extinct completely. When the death rate of consumers exceeds their growth rate, both consumers and predators will die out, leaving only producers to survive. Conversely, when the growth rate of consumers exceeds their death rate, while predators experience the opposite, then both producers and consumers can coexist.

Our findings also show that light intensity plays a crucial role in shaping population dynamics by impacting producer nutrient levels and carbon synthesis. Numerical analysis reveals that as light intensity varies, the system demonstrates quasi-symmetric dynamics. In the absence of the fear effect ($\rho = 0$), the system exhibits dynamics similar to those observed in [5]. As light intensity transitions from extremely low or extremely strong to intermediate levels, the system undergoes a sequence of states, including a producer-only state, a producer-consumer state, a coexistence stable state, periodic oscillations, and chaos. This implies that excessively high or low light intensity is detrimental to biodiversity, while moderate light intensity allows for the coexistence of all three species.

However, with the magnitude of the fear effect increasing, chaos gradually diminishes, indicating that fear effect stabilizes the system, which aligns with previous

studies [65, 41, 52, 29, 1, 36]. Moreover, as the fear effect increases, the system undergoes a transition from chaotic to periodic dynamics and eventually reaches an equilibrium state. This further confirms our conclusion.

Beyond stability, the fear effect has diverse impacts on different trophic populations. A low fear effect promotes producer growth and decreases grazer growth; however, predators consistently benefit from increasing fear effect, even at higher levels. Additionally, at higher fear effect levels, an increase in fear promotes mean trophic energy transfer efficiency.

Furthermore, we demonstrate that fear effect amplifies the effects of food quality on consumers. When the food quality is high ($Q > \bar{Q}$), the presence of the fear effect enhances the production efficiency of consumers. Conversely, when food quality is poor ($Q < \bar{Q}$), the fear effect exacerbates the decline in production efficiency caused by low-nutrient food. This finding is consistent with experimental observations [4]. The presence of indirect predation risk from predators can influence key life-history responses in consumers, such as increased nutrient demand [53], accelerating reproduction at a smaller size [3], and enhancing consumer agility [66], which improves chances of escaping actual predation. When combined with high-quality food, these adaptations lead to higher survival rates for consumers. However, in nutrient-limited environments, the fear effect may further exacerbate the challenges imposed by stoichiometric constraints, potentially leading to population declines or even extinction.

In this paper, we focused on the stoichiometry-dependent fear effect in a simple three-dimensional food chain. However, predator-prey interactions in natural communities are far more complex. For instance, intraspecific competition among predators or prey is commonly observed [7], and extremely strong competition may cause the extinction of weaker species. Several recent studies have explored the fear effect on predator-prey systems with intraspecific competition [39, 51, 40, 1]. Additionally, middle predators may also exert fear effects on their prey, as studied in [41, 8]. Considering that the fear effect is highly dependent on food quality, further exploration of the influence of food quality on these intricate predator-prey interactions may provide valuable insights for better understanding population dynamics. Moreover, in addition to food quality, the behavioral response of prey to indirect predation risk can also be influenced by other internal factors, including their fitness state, size, and age [54, 25, 37]. Incorporating these essential factors in future research may contribute to a more realistic understanding of predator-prey dynamics and the role of fear in shaping ecological communities.

Appendix A. Well-definedness.

A.1. Proof of Theorem 3.1.

Proof. $x'(t)$ is well defined as $x \to 0$, since

$$\frac{\mathrm{d}x}{\mathrm{d}t} = bx\left(1 - \frac{x}{\min\left\{K, \frac{P-\theta_y y-\theta_z z}{Q_m}\right\}}\right) - f(x)y.$$

From system (2.4), we have

$$\frac{\mathrm{d}y}{\mathrm{d}t} = h(z,Q)\min\Big\{1,\frac{Q}{\theta_y}\Big\}f(x)y - g(y)z - d_y y$$

$$= \begin{cases} \left(\rho\dfrac{P-\theta_y y-\theta_z z-\bar{Q}x}{P-\theta_y y-\theta_z z+\gamma x}\dfrac{z}{z+\beta}+\bar{e}_y\right)f(x)y - g(y)z - d_y y, \\ \qquad\qquad\qquad\qquad\qquad\qquad\qquad\qquad \theta_y x+\theta_y y+\theta_z z < P, \\ \left(\rho\dfrac{P-\theta_y y-\theta_z z-\bar{Q}x}{P-\theta_y y-\theta_z z+\gamma x}\dfrac{z}{z+\beta}+\bar{e}_y\right)\dfrac{P-\theta_y y-\theta_z z}{\theta_y}\dfrac{f(x)}{x}y - g(y)z - d_y y, \\ \qquad\qquad\qquad\qquad\qquad\qquad\qquad\qquad \theta_y x+\theta_y y+\theta_z z > P. \end{cases}$$

Since $\frac{f(x)}{x}$ satisfies $\left(\frac{f(x)}{x}\right)' < 0$ for $x > 0$ and $\lim\limits_{x\to 0}\frac{f(x)}{x} = f'(0) < \infty$, then $y'(t)$ is well defined at $x \to 0$. This completes the proof. ∎

A.2. Proof of Theorem 3.2.

Proof. Assume $S(t) = (x(t), y(t), z(t))$ is a solution of system (2.4) with $S(0) \in \Omega$ and t_1 is the first time that $S(t)$ touches or crosses the boundary of Ω. We will prove the theorem by contradiction arguments from five cases.

Case 1. $x(t_1) = 0$. Let $f'(0) = \lim\limits_{x\to 0}\frac{f(x)}{x}$, and $\bar{y} = \max\limits_{t\in[0,t_1]} y(t) \le \frac{P}{\theta_y}$.

Then $\forall t \in [0, t_1]$, we have

$$\frac{\mathrm{d}x}{\mathrm{d}t} \ge -f(x)y \ge -\max_{t\in[0,t_1]}\frac{f(x)}{x}\bar{y}x = \delta_1 x,$$

where δ_1 is a constant. Thus, $x(t_1) \ge x(0)e^{\delta_1 t_1} > 0$ holds, which contradicts with $x(t_1) = 0$. Therefore, $S(t_1)$ can not reach this boundary.

Case 2. $y(t_1) = 0$.

Let $g'(0) = \lim\limits_{y\to 0}\frac{g(y)}{y}$, and $\bar{z} = \max\limits_{t\in[0,t_1]} z(t) \le \frac{P}{\theta_z}$.

$\forall t \in [0, t_1]$, it follows that

$$\frac{\mathrm{d}y}{\mathrm{d}t} \ge -g(y)z - d_y y \ge -\left(\max_{t\in[0,t_1]}\frac{g(y)}{y}\bar{z} + d_y\right)y = \delta_2 y,$$

where δ_2 is a constant. Thus, $y(t_1) \ge y(0)e^{\alpha_2 t_1} > 0$ holds, which contradicts with $y(t_1) = 0$. Therefore, $S(t_1)$ can not reach this boundary.

Case 3. $z(t_1) = 0$.

$\forall t \in [0, t_1]$, it follows that

$$\frac{\mathrm{d}z}{\mathrm{d}t} = e_z\min\Big\{1,\frac{\theta_y}{\theta_z}\Big\}g(y)z - d_z z \ge -d_z z = \delta_3 z,$$

where δ_3 is a constant. Thus, $z(t_1) \ge z(0)e^{\delta_3 t_1} > 0$ holds, which contradicts with $z(t_1) = 0$. Therefore, $S(t_1)$ can not reach this boundary.

Case 4. $Q_m x(t_1) + \theta_y y(t_1) + \theta_z z(t_1) = P$, i.e., $Q(t_1) = \frac{P-\theta_y y(t_1)-\theta_z z(t_1)}{x(t_1)} = Q_m$. It follows that

$$bx(t_1)\left(1 - \frac{x(t_1)}{\min\Big\{K, \frac{P-\theta_y y(t_1)-\theta_z z(t_1)}{Q_m}\Big\}}\right) = bx(t_1)\left(1 - \frac{x(t_1)}{\min\{K, x(t_1)\}}\right) \le 0.$$

Since $e_z < 1$ and $h(z(t_1), Q_m) < 1$, we have

$$\begin{aligned}&\left.\frac{\mathrm{d}(Q_m x + \theta_y y + \theta_z z)}{\mathrm{d}t}\right|_{t=t_1}\\ \le& y(t_1)[(h(z(t_1), Q_m)\min\{\theta_y, Q_m\} - Q_m)f(x(t_1)) - \theta_y d_y] + z(t_1)[(e_z \min\{\theta_y, \theta_z\}\\ &- \theta_y)g(y(t_1)) - \theta_z d_z] \le 0.\end{aligned}$$

This implies that $S(t_1)$ can not cross this boundary.

Case 5. $x(t_1) = k$, where $k = \min\left\{K, \frac{P}{Q_m}\right\}$. It follows that

$$\left.\frac{\mathrm{d}x}{\mathrm{d}t}\right|_{t=t_1} \le bx(t_1)\left(1 - \frac{x(t_1)}{\min\left\{K, \frac{P}{Q_m}\right\}}\right) = bx(t_1)\left(1 - \frac{x(t_1)}{k}\right) = 0.$$

Therefore, $S(t_1)$ can not cross this boundary.

In summary, the solution $S(t)$ of system (2.4) starting from Ω will stay in Ω for all forward time. ∎

Appendix B. Analysis of equilibria. To simplify the analysis, we rewrite system (2.4) in the following form:

$$\begin{cases}\dfrac{\mathrm{d}x}{\mathrm{d}t} = xF(x, y, z),\\ \dfrac{\mathrm{d}y}{\mathrm{d}t} = yG(x, y, z),\\ \dfrac{\mathrm{d}z}{\mathrm{d}t} = zH(x, y, z),\end{cases} \tag{B.1}$$

where

$$\begin{aligned}F(x, y, z) &= b\left(1 - \frac{x}{\min\left\{K, \frac{P-\theta_y y-\theta_z z}{Q_m}\right\}}\right) - \frac{f(x)}{x}y,\\ G(x, y, z) &= h(z, Q)\min\left\{1, \frac{Q}{\theta_y}\right\}f(x) - \frac{g(y)}{y}z - d_y,\\ H(x, y, z) &= e_z \min\left\{1, \frac{\theta_y}{\theta_z}\right\}g(y) - d_z.\end{aligned}$$

The boundary equilibria are $E_0(0, 0, 0)$, $E_1(k, 0, 0)$, and $E_2(\bar{x}, \bar{y}, 0)$. We consider the Jacobian matrix of system (B.1) to study the local stability of the equilibria.

B.1. Proof of Theorem 3.3.

Proof. At $E_0(0, 0, 0)$, the Jacobian matrix is given by

$$J(E_0) = \begin{pmatrix} b & 0 & 0\\ 0 & -d_y & 0\\ 0 & 0 & -d_z\end{pmatrix}.$$

Since the eigenvalues have different signs, E_0 is unstable. ∎

B.2. Proof of Theorem 3.4.

Proof. At $E_1(k,0,0)$, the Jacobian matrix is given by

$$J(E_1) = \begin{pmatrix} -b & kF_y(k,0,0) & kF_z(k,0,0) \\ 0 & \bar{e}_y \min\left\{1, \frac{P}{k\theta_y}\right\} f(k) - d_y & 0 \\ 0 & 0 & -d_z \end{pmatrix}.$$

If $\bar{e}_y \min\left\{1, \frac{P}{k\theta_y}\right\} f(k) \geq d_y$, then E_1 is unstable; otherwise, E_1 is LAS. ∎

B.3. Complementary analysis of existence of E_2. To show conditions for the existence of equilibrium E_2, we follow the terminologies in [34, 46, 5]. The boundary equilibrium $E_2(\bar{x}, \bar{y}, 0)$ can be viewed as internal equilibrium of the two-dimensional subsystem without predators. Therefore, it is sufficient to study the stability of E_2 in x-y plane. We separate region Ω in x-y plane into two parts by the line $x+y = \frac{P}{\theta_y}$. The lower region and upper region are denoted as I and II respectively in Figure 12.

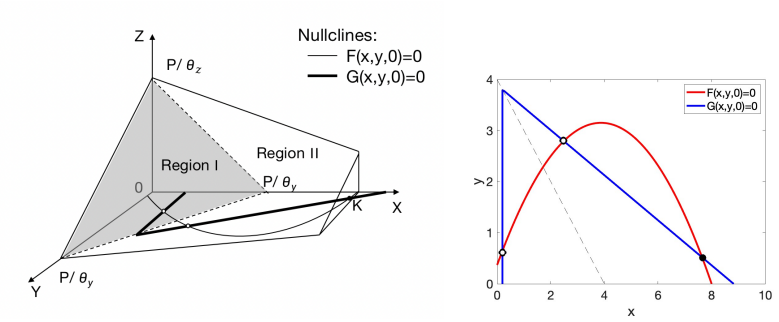

(a) (b)

Fig. 12: (a) The producer nullcline $F(x,y,0) = 0$ (parabola) and the consumer nullcline $G(x,y,0) = 0$ (peak-shaped curve) in x-y plane for the truncated triangular pyramid case. (b) The nullclines for the producer-consumer system as $K = 8$. The solid circles denote stable equilibria and open circles represent unstable equilibria.

The nullclines of consumers consist of three curves $x = f^{-1}(\frac{d_y}{\bar{e}_y})$, $y = -\frac{d_y}{\bar{e}_y}\frac{x}{f(x)} + \frac{P}{\theta_y}$, and $y = 0$ as Figure 12. Clearly, there is a peak at the intersection of $x = f^{-1}(\frac{d_y}{\bar{e}_y})$ and $y = -\frac{d_y}{\bar{e}_y}\frac{x}{f(x)} + \frac{P}{\theta_y}$. Therefore, E_2 must satisfy

$$\bar{y} \leq \bar{y}_{\max} = \frac{P}{\theta_y} - f^{-1}\left(\frac{d_y}{\bar{e}_y}\right).$$

B.4. Proof of Theorem 3.5.

Proof. To analyze the local stability of E_2, we apply the method of Jacobian matrix as in [34]. The Jacobian matrix of $E_2(\bar{x}, \bar{y}, 0)$ is given by

$$J(E_2) = \begin{pmatrix} J_{\text{sub}} & J_1 \\ (0,0) & H(\bar{x}, \bar{y}, 0) \end{pmatrix},$$

where J_1 is a 2x1 matrix, and

$$J_{\text{sub}} = \begin{pmatrix} \bar{x}F_{1_x}(\bar{x},\bar{y}) & \bar{x}F_{1_y}(\bar{x},\bar{y}) \\ \bar{y}G_{1_x}(\bar{x},\bar{y}) & \bar{y}G_{1_y}(\bar{x},\bar{y}) \end{pmatrix}.$$

Note that the sign of eigenvalues of matrix $J(E_2)$ depends only on the sign of $H(\bar{x},\bar{y},0)$ and eigenvalues of J_{sub}. Therefore, we can disregard J_1 when studying the stability of E_2.

Here,

$$F_{1_x} = -\frac{b}{\min\{K, \frac{P-\theta_y y}{Q_m}\}} - \left(\frac{f(x)}{x}\right)' y,$$

$$F_{1_y} = \begin{cases} -\dfrac{f(x)}{x} < 0, & y \le \frac{P-Q_m K}{\theta_y}, \\ -\dfrac{bQ_m\theta_y x}{(P-\theta_y y)^2} - \dfrac{f(x)}{x} < 0, & y > \frac{P-Q_m K}{\theta_y}, \end{cases}$$

$$G_{1_x} = \begin{cases} \bar{e}_y f'(x) > 0, & x+y < \frac{P}{\theta_y}, \\ \bar{e}_y \dfrac{P-\theta_y y}{\theta_y}\left(\dfrac{f(x)}{x}\right)' < 0, & x+y > \frac{P}{\theta_y}, \end{cases}$$

$$G_{1_y} = \begin{cases} 0, & x+y < \frac{P}{\theta_y}, \\ -\bar{e}_y \dfrac{f(x)}{x} < 0, & x+y > \frac{P}{\theta_y}. \end{cases}$$

Hence, the trace and determinant of J_{sub} are given by

$$\text{Tr}(J_{\text{sub}}) = \bar{x}F_{1_x} + \bar{y}G_{1_y},$$
$$\text{Det}(J_{\text{sub}}) = \bar{x}\bar{y}(F_{1_x}G_{1_y} - F_{1_y}G_{1_x}).$$

The slopes of the producer and consumer nullclines at (x,y) are defined by $-F_{1_x}/F_{1_y}$ and $-G_{1_x}/G_{1_y}$, respectively. We consider the following two cases:

Case1: When (x,y) is in region I, i.e., $x+y < \frac{P}{\theta_y}$.

At E_2, $G_{1_x} > 0$, $G_{1_y} = 0$ and $F_{1_y} < 0$. It follows that

$$\text{Det}(J_{\text{sub}}) > 0,$$
$$\text{sign}(\text{Tr}(J_{\text{sub}})) = \text{sign}(F_{1_x}) = \text{sign}\left(-\frac{F_{1_x}}{F_{1_y}}\right).$$

If the producer nullcline is decreasing at E_2, then $\text{Tr}(J_{\text{sub}}) < 0$ and E_2 is LAS. If the producer nullcline is increasing at E_2, then $\text{Tr}(J_{\text{sub}}) > 0$ and E_2 is unstable.

Case2: When (x,y) is in region II, i.e., $x+y > \frac{P}{\theta_y}$.

At E_2, $G_{1_x} < 0$, $G_{1_y} < 0$ and $F_{1_y} < 0$. It follows that

$$\text{sign}(\text{Det}(J_{\text{sub}})) = \text{sign}\left(\frac{F_{1_x}G_{1_y} - G_{1_x}F_{1_y}}{F_{1_y}G_{1_y}}\right) = \text{sign}\left(-\frac{G_{1_x}}{G_{1_y}} - \left(-\frac{F_{1_x}}{F_{1_y}}\right)\right).$$

Therefore, at E_2, if the slope of the consumer nullcline is less than the slope of the producer nullcline, i.e., $-\frac{G_{1_x}}{G_{1_y}} < -\frac{F_{1_x}}{F_{1_y}}$, then $\text{Det}(J_{\text{sub}}) < 0$ and E_2 is unstable. If the slope of the consumer nullcline is higher than the slope of the producer nullcline, i.e., $0 > -\frac{G_{1_x}}{G_{1_y}} > -\frac{F_{1_x}}{F_{1_y}}$, then $\text{Det}(J_{\text{sub}}) > 0$, $F_{1_x} < 0$, $\text{Tr}(J_{\text{sub}}) < 0$. Hence, E_2 is LAS. □

B.5. Proof of Theorem 3.6.

Proof. We prove this theorem by constructing a Lyapunov function. Consider

$$\begin{aligned} L(x,y,z) =&\alpha_1\left(x-x^*-x^*\ln\left(\frac{x}{x^*}\right)\right)+\alpha_2\left(y-y^*-y^*\ln\left(\frac{y}{y^*}\right)\right)\\ &+\alpha_3\left(z-z^*-z^*\ln\left(\frac{z}{z^*}\right)\right), \end{aligned}$$

for any $(x,y,z)\in\Omega$. It is easy to prove that L is positive definite. Differentiating L with respect to t, we have

$$\begin{aligned} &\frac{\mathrm{d}L(x(t),y(t),z(t))}{\mathrm{d}t}\\ =&\alpha_1\left(1-\frac{x^*}{x}\right)\frac{\mathrm{d}x}{\mathrm{d}t}+\alpha_2\left(1-\frac{y^*}{y}\right)\frac{\mathrm{d}y}{\mathrm{d}t}+\alpha_3\left(1-\frac{z^*}{z}\right)\frac{\mathrm{d}z}{\mathrm{d}t}\\ =&\left[\alpha_1 bx-\frac{\alpha_1 bx^2}{\min\left\{K,\frac{P-\theta_y y-\theta_z z}{Q_m}\right\}}-\alpha_1 f(x)y-\alpha_1 bx^*+\frac{\alpha_1 bx^*x}{\min\left\{K,\frac{P-\theta_y y-\theta_z z}{Q_m}\right\}}\right.\\ &\left.+\alpha_1\frac{x^*}{x}f(x)y\right]+\left[\alpha_2 h(z,Q)\min\left\{1,\frac{Q}{\theta_y}\right\}f(x)y-\alpha_2 g(y)z-d_y\alpha_2 y\right.\\ &\left.-\alpha_2 y^* h(z,Q)\min\left\{1,\frac{Q}{\theta_y}\right\}f(x)+\alpha_2\frac{y^*}{y}g(y)z+d_y\alpha_2 y^*\right]\\ &+\left[\alpha_3 e_z\min\left\{1,\frac{\theta_y}{\theta_z}\right\}g(y)z-\alpha_3 d_z z-\alpha_3 z^* e_z\min\left\{1,\frac{\theta_y}{\theta_z}\right\}g(y)+\alpha_3 d_z z^*\right]\\ =&\left[\alpha_2 h(z,Q)\min\left\{1,\frac{Q}{\theta_y}\right\}f(x)y-\alpha_1 f(x)y\right]+\left[\alpha_3 e_z\min\left\{1,\frac{\theta_y}{\theta_z}\right\}g(y)z-\alpha_2 g(y)z\right]\\ &+\left[\alpha_1\frac{x^*}{x}f(x)y-d_y\alpha_2 y-\alpha_3 z^* e_z\min\left\{1,\frac{\theta_y}{\theta_z}\right\}g(y)\right]+\left[\alpha_2\frac{y^*}{y}g(y)z-\alpha_3 d_z z\right]\\ &+\left[\alpha_1 b(x-x^*)-\frac{\alpha_1 b(x^2-x^*x)}{\min\left\{K,\frac{P-\theta_y y-\theta_z z}{Q_m}\right\}}-\alpha_2 y^* h(z,Q)\min\left\{1,\frac{Q}{\theta_y}\right\}f(x)\right.\\ &\left.+d_y\alpha_2 y^*+\alpha_3 d_z z^*\right]\\ =:&\,\mathcal{J}_1+\mathcal{J}_2+\mathcal{J}_3+\mathcal{J}_4+\mathcal{J}_5. \end{aligned}$$

Let $\alpha_3=1$, $\alpha_2=e_z\min\left\{1,\frac{\theta_y}{\theta_z}\right\}$, and $\alpha_1=e_y\alpha_2$. It follows that

$$\begin{aligned} &\mathcal{J}_1=\alpha_2\left(h(z,Q)\min\left\{1,\frac{Q}{\theta_y}\right\}-e_y\right)f(x)y\le 0,\\ &\mathcal{J}_2=\alpha_2 g(y)z-\alpha_2 g(y)z=0,\\ &\mathcal{J}_3=\alpha_2\left(\frac{e_y x^* c_1}{a_1+x}-d_y-\frac{c_2 z^*}{a_2+y}\right)y\le\alpha_2\left(\frac{e_y x^* c_1}{a_1}-d_y-\frac{c_2 z^*}{a_2+P/\theta_y}\right)y. \end{aligned}$$

Thus, if $L_1\le 0$, then $\mathcal{J}_3\le 0$ holds.

Furthermore, $\mathcal{J}_4$ satisfies

$$\mathcal{J}_4=\alpha_2\frac{y^*}{y}\frac{c_2 y}{a_2+y}z-d_z z\le\left(\frac{\alpha_2 y^* c_2}{a_2}-d_z\right)z=\left(\frac{e_z\min\left\{1,\frac{\theta_y}{\theta_z}\right\}y^* c_2}{a_2}-d_z\right)z.$$

Thus if $L_2 \leq 0$, then $\mathcal{J}_4 \leq 0$ holds.

For $\mathcal{J}_5$, we have

$$\begin{aligned}\mathcal{J}_5 =& -\frac{\alpha_1 b}{\min\Big\{K, \frac{P-\theta_y y-\theta_z z}{Q_m}\Big\}}x^2 + \left[\alpha_1 b + \frac{\alpha_1 b x^*}{\min\Big\{K, \frac{P-\theta_y y-\theta_z z}{Q_m}\Big\}}\right.\\ &\left. -\alpha_2 y^* h(z,Q)\min\Big\{1, \frac{Q}{\theta_y}\Big\}\frac{a_1}{c_1+x}\right]x + (-\alpha_1 b x^* + d_y\alpha_2 y^* + \alpha_3 d_z z^*)\\ =:& -Ax^2 + Bx + C.\end{aligned}$$

Note that $A > 0$, then $\mathcal{J}_5 \leq 0$ for all $x \in \Omega$ if and only if $C \leq 0$ and $-Ak^2+Bk+C \leq 0$.

Apparently, $C \leq 0$ if and only if $L_3 \leq 0$.

Moreover, by assumption (A3), we have

$$\begin{aligned}&-Ak^2 + Bk + C\\ \leq& -\frac{\alpha_1 b k^2}{K} + \left[\alpha_1 b + \frac{\alpha_1 b x^*}{\min\Big\{K, \frac{P_m}{Q_m}\Big\}} - \alpha_2 y^* h_m \min\Big\{1, \frac{Q_m}{\theta_y}\Big\}\frac{a_1}{c_1+k}\right]k + (-\alpha_1 b x^*\\ &+ d_y\alpha_2 y^* + \alpha_3 d_z z^*)\\ =& e_z \min\Big\{1, \frac{\theta_y}{\theta_z}\Big\}\left[\left(\frac{k}{\min\Big\{K, \frac{P_m}{Q_m}\Big\}} - 1\right)e_y b x^* + (d_y\right.\\ &\left. -h_m \min\Big\{1, \frac{Q_m}{\theta_y}\Big\}\frac{a_1}{c_1+k}k\right)y^* + \left(1 - \frac{k}{K}\right)e_y b k\right] + d_z z^*.\end{aligned}$$

Thus, if $L_4 \leq 0$, then $-Ak^2 + Bk + C \leq 0$.

Therefore, if conditions $L_i \leq 0$ for $i = 1, 2, 3, 4$ hold, with at least one of these inequalities being strictly negative, then $\frac{\mathrm{d}L}{\mathrm{d}t} < 0$. It follows that the internal equilibrium E^* is GAS. This completes the proof. ∎

Data Availability Statement. The data that support the findings of this study are available from the authors upon reasonable request.

Conflict of interest. The authors declare that they have no conflict of interest.

REFERENCES

[1] N. Ali, *On the food chain model with prey refuge and fear effect*, Int. J. Nonlinear Anal. Appl., 13 (2022), pp. 2071–2086.

[2] T. Andersen, *Pelagic nutrient cycles: herbivores as sources and sinks*, vol. 129, Springer Science & Business Media, 2013.

[3] S. L. Ball and R. L. Baker, *Predator–induced life history changes: Antipredator behavior costs or facultative life history shifts?*, Ecology, 77 (1996), pp. 1116–1124.

[4] A. T. Bell, D. L. Murray, C. Prater, and P. C. Frost, *Fear and food: Effects of predator-derived chemical cues and stoichiometric food quality on daphnia*, Limnol. Oceanogr., 64 (2019), pp. 1706–1715.

[5] M. Chen, M. Fan, and Y. Kuang, *Global dynamics in a stoichiometric food chain model with two limiting nutrients*, Math. Biosci., 289 (2017), pp. 9–19.

[6] M. Chen, Y. Takeuchi, and J. Zhang, *Dynamic complexity of a modified leslie-gower predator-prey system with fear effect*, Commun. Nonlinear Sci. Numer. Simul., (2023), p. 107109.

[7] M. E. Clark, T. G. Wolcott, D. L. Wolcott, and A. H. Hines, *Intraspecific interference among foraging blue crabs callinectes sapidus: interactive effects of predator density and prey patch distribution*, Mar. Ecol. Prog. Ser., 178 (1999), pp. 69–78.

[8] P. Cong, M. Fan, and X. Zou, *Dynamics of a three-species food chain model with fear effect*, Commun. Nonlinear Sci. Numer. Simul., 99 (2021), p. 105809.
[9] J. P. DeLong and M. Walsh, *The interplay between resource supply and demand determines the influence of predation on prey body size*, Can. J. Fish. Aquat. Sci., 73 (2016), pp. 709–715.
[10] W. R. DeMott and E. Van Donk, *Strong interactions between stoichiometric constraints and algal defenses: evidence from population dynamics of daphnia and algae in phosphorus-limited microcosms*, Oecologia, 171 (2013), pp. 175–186.
[11] C. M. Duarte, *Nutrient concentration of aquatic plants: patterns across species*, Limnol. Oceanogr., 37 (1992), pp. 882–889.
[12] P. Eklöv and C. Halvarsson, *The trade-off between foraging activity and predation risk for rana temporaria in different food environments*, Can. J. Zool., 78 (2000), pp. 734–739.
[13] J. J. Elser, E. R. Marzolf, and C. R. Goldman, *Phosphorus and nitrogen limitation of phytoplankton growth in the freshwaters of north america: a review and critique of experimental enrichments*, Can. J. Fish. Aquat. Sci., 47 (1990), pp. 1468–1477.
[14] K. M. Fagerbakke, M. Heldal, and S. Norland, *Content of carbon, nitrogen, oxygen, sulfur and phosphorus in native aquatic and cultured bacteria*, Aquat. Microb. Ecol., 10 (1996), pp. 15–27.
[15] M. C. Ferrari, M. I. McCormick, B. J. Allan, R. Choi, R. A. Ramasamy, J. L. Johansen, M. D. Mitchell, and D. P. Chivers, *Living in a risky world: the onset and ontogeny of an integrated antipredator phenotype in a coral reef fish*, Sci. Rep., 5 (2015), p. 15537.
[16] M. C. Ferrari, B. D. Wisenden, and D. P. Chivers, *Chemical ecology of predator-prey interactions in aquatic ecosystems: a review and prospectus*, Can. J. Zool., 88 (2010), pp. 698–724.
[17] M. E. Fraker, *The dynamics of predation risk assessment: responses of anuran larvae to chemical cues of predators*, J. Anim. Ecol., 77 (2008), pp. 638–645.
[18] M. Ghosh and N. Chattopadhyay, *Effects of carbon/nitrogen/phosphorus ratio on mineralizing bacterial population in aquaculture systems*, J. Appl. Aquac., 17 (2005), pp. 85–98.
[19] R. D. Guariento and F. d. A. Esteves, *The several faces of fear: ecological consequences of predation risk in a lagoon model system*, Acta Limnol. Bras., 25 (2013), pp. 211–223.
[20] M. Haapakoski, A. Hardenbol, and K. D. Matson, *Exposure to chemical cues from predator-exposed conspecifics increases reproduction in a wild rodent*, Sci. Rep., 8 (2018), pp. 1–9.
[21] A. Hastings and T. Powell, *Chaos in a three-species food chain*, Ecology, 72 (1991), pp. 896–903.
[22] X. He and J. F. Kitchell, *Direct and indirect effects of predation on a fish community: a whole-lake experiment*, Trans. Am. Fish. Soc., 119 (1990), pp. 825–835.
[23] R. Hecky and P. Kilham, *Nutrient limitation of phytoplankton in freshwater and marine environments: a review of recent evidence on the effects of enrichment 1*, Limnol. Oceanogr., 33 (1988), pp. 796–822.
[24] M. R. Heithaus and L. M. Dill, *Food availability and tiger shark predation risk influence bottlenose dolphin habitat use*, Ecology, 83 (2002), pp. 480–491.
[25] M. R. Heithaus, A. Frid, A. J. Wirsing, L. M. Dill, J. W. Fourqurean, D. Burkholder, J. Thomson, and L. Bejder, *State-dependent risk-taking by green sea turtles mediates top-down effects of tiger shark intimidation in a marine ecosystem*, J. Anim. Ecol., 76 (2007), pp. 837–844.
[26] P. D. Jeyasingh, J. M. Goos, S. K. Thompson, C. M. Godwin, and J. B. Cotner, *Ecological stoichiometry beyond redfield: An ionomic perspective on elemental homeostasis*, Front. Microbiol., 8 (2017), p. 722.
[27] J. Ji, R. Milne, and H. Wang, *Stoichiometry and environmental change drive dynamical complexity and unpredictable switches in an intraguild predation model*, J. Math. Biol., 86 (2023), p. 31.
[28] S. E. Jørgensen, S. N. Nielsen, L. A. Jørgensen, et al., *Handbook of ecological parameters and ecotoxicology*, Elsevier, 1991.
[29] R. P. Kaur, A. Sharma, and A. K. Sharma, *Impact of fear effect on plankton-fish system dynamics incorporating zooplankton refuge*, Chaos Solit. Fractals, 143 (2021), p. 110563.
[30] B. Kesavaraju, K. Damal, and S. A. Juliano, *Threat-sensitive behavioral responses to concentrations of water-borne cues from predation*, Ethology, 113 (2007), pp. 199–206.
[31] C. Laird, *Effects of Phosphorus Concentration on Algal Composition and Bioprocessing Potential*, PhD thesis, Clemson University, 2018.
[32] S. J. Leroux and O. J. Schmitz, *Predator-driven elemental cycling: The impact of predation and risk effects on ecosystem stoichiometry*, Ecol. Evol., 5 (2015), pp. 4976–4988.
[33] X. Li, H. Wang, and Y. Kuang, *Global analysis of a stoichiometric producer–grazer model*

with holling type functional responses, J. Math. Biol., 63 (2011), pp. 901–932.
[34] I. Loladze, Y. Kuang, and J. J. Elser, *Stoichiometry in producer-grazer systems: linking energy flow with element cycling*, Bull. Math. Biol., 62 (2000), pp. 1137–1162.
[35] U. Magnea, R. Sciascia, F. Paparella, R. Tiberti, and A. Provenzale, *A model for high-altitude alpine lake ecosystems and the effect of introduced fish*, Ecological modelling, 251 (2013), pp. 211–220.
[36] G. Mandal, N. Ali, L. N. Guin, and S. Chakravarty, *Impact of fear on a tri-trophic food chain model with supplementary food source*, Int. J. Dyn. Control, (2023), pp. 1–34.
[37] C. M. Matassa and G. C. Trussell, *Prey state shapes the effects of temporal variation in predation risk*, Proc. R. Soc. B: Biol. Sci., 281 (2014), p. 20141952.
[38] M. D. Mitchell and A. R. Harborne, *Non-consumptive effects in fish predator-prey interactions on coral reefs*, Coral Reefs, 39 (2020), pp. 867–884.
[39] D. Mukherjee, *Role of fear in predator-prey system with intraspecific competition*, Math. Comput. Simul., 177 (2020), pp. 263–275.
[40] D. Mukherjee, *Effect of fear on two predator-one prey model in deterministic and fluctuating environment*, Math. Appl. Sci. Eng., 2 (2021), pp. 55–71.
[41] P. Panday, N. Pal, S. Samanta, and J. Chattopadhyay, *Stability and bifurcation analysis of a three-species food chain model with fear*, Int. J. Bifurc. Chaos, 28 (2018), p. 1850009.
[42] K. Pauwels, R. Stoks, and L. De Meester, *Enhanced anti-predator defence in the presence of food stress in the water flea daphnia magna*, Funct. Ecol., 24 (2010), pp. 322–329.
[43] A. Peace, *Effects of light, nutrients, and food chain length on trophic efficiencies in simple stoichiometric aquatic food chain models*, Ecol. Model., 312 (2015), pp. 125–135.
[44] A. Peace and H. Wang, *Compensatory foraging in stoichiometric producer–grazer models*, Bull. Math. Biol., 81 (2019), pp. 4932–4950.
[45] A. Peace, H. Wang, and Y. Kuang, *Dynamics of a producer–grazer model incorporating the effects of excess food nutrient content on grazer's growth*, Bull. Math. Biol., 76 (2014), pp. 2175–2197.
[46] A. Peace, Y. Zhao, I. Loladze, J. J. Elser, and Y. Kuang, *A stoichiometric producer-grazer model incorporating the effects of excess food-nutrient content on consumer dynamics*, Math. Biosci., 244 (2013), pp. 107–115.
[47] A. Pilati and M. J. Vanni, *Ontogeny, diet shifts, and nutrient stoichiometry in fish*, Oikos, 116 (2007), pp. 1663–1674.
[48] E. L. Preisser, D. I. Bolnick, and M. F. Benard, *Scared to death? the effects of intimidation and consumption in predator-prey interactions*, Ecology, 86 (2005), pp. 501–509.
[49] M. M. Rana, C. Dissanayake, L. Juan, K. R. Long, and A. Peace, *Mechanistically derived spatially heterogeneous producer-grazer model subject to stoichiometric constraints*, Math. Biosci. Eng., 16 (2019), pp. 222–233, https://doi.org/10.3934/mbe.2019012.
[50] R. A. Relyea, *How prey respond to combined predators: a review and an empirical test*, Ecology, 84 (2003), pp. 1827–1839.
[51] D. Sahoo and G. Samanta, *Impact of fear effect in a two prey-one predator system with switching behaviour in predation*, Differ. Equ. Dyn. Syst., (2021), pp. 1–23.
[52] K. Sarkar and S. Khajanchi, *Impact of fear effect on the growth of prey in a predator-prey interaction model*, Ecol. Complex., 42 (2020), p. 100826.
[53] O. J. Schmitz and G. C. Trussell, *Multiple stressors, state-dependence and predation risk—foraging trade-offs: toward a modern concept of trait-mediated indirect effects in communities and ecosystems*, Curr. Opin. Behav. Sci., 12 (2016), pp. 6–11.
[54] T. Stankowich and D. T. Blumstein, *Fear in animals: a meta-analysis and review of risk assessment*, Proc. R. Soc. B: Biol. Sci., 272 (2005), pp. 2627–2634.
[55] R. W. Sterner and J. J. Elser, *Ecological stoichiometry*, Princeton university press, 2017.
[56] H. Stibor, *Predator induced life-history shifts in a freshwater cladoceran*, Oecologia, 92 (1992), pp. 162–165.
[57] E. F. Stoermer, B. G. Ladewski, and C. L. Schelske, *Population responses of lake michigan phytoplankton to nitrogen and phosphorus enrichment*, Hydrobiologia, 57 (1978), pp. 249–265.
[58] W. Tang, H. Guo, C. C. Baskin, W. Xiong, C. Yang, Z. Li, H. Song, T. Wang, J. Yin, X. Wu, et al., *Effect of light intensity on morphology, photosynthesis and carbon metabolism of alfalfa (medicago sativa) seedlings*, Plants, 11 (2022), p. 1688.
[59] A. A. Thirthar, S. J. Majeed, K. Shah, and T. Abdeljawad, *The dynamics of an aquatic ecological model with aggregation, fear and harvesting effects*, AIMS Math., 7 (2022), pp. 18532–18552.
[60] J. Urabe and R. W. Sterner, *Regulation of herbivore growth by the balance of light and nutrients.*, Proc. Natl. Acad. Sci., 93 (1996), pp. 8465–8469.

[61] M. Van Dievel, L. Janssens, and R. Stoks, *Short-and long-term behavioural, physiological and stoichiometric responses to predation risk indicate chronic stress and compensatory mechanisms*, Oecologia, 181 (2016), pp. 347–357.
[62] H. Wang, Y. Kuang, and I. Loladze, *Dynamics of a mechanistically derived stoichiometric producer-grazer model*, J. Biol. Dyn., 2 (2008), pp. 286–296.
[63] H. Wang, Z. Lu, and A. Raghavan, *Weak dynamical threshold for the "strict homeostasis" assumption in ecological stoichiometry*, Ecol. Model., 384 (2018), pp. 233–240.
[64] H. Wang, R. W. Sterner, and J. J. Elser, *On the "strict homeostasis" assumption in ecological stoichiometry*, Ecol. Model., 243 (2012), pp. 81–88.
[65] X. Wang, L. Zanette, and X. Zou, *Modelling the fear effect in predator-prey interactions*, J. Math. Biol., 73 (2016), pp. 1179–1204.
[66] J. Wen and T. Ueno, *Predator cue-induced plasticity of morphology and behavior in planthoppers facilitate the survival from predation*, Sci. Rep., 11 (2021), p. 16760.
[67] T. Xie, X. Yang, X. Li, and H. Wang, *Complete global and bifurcation analysis of a stoichiometric predator-prey model*, J. Dyn. Differ. Equ., 30 (2018), pp. 447–472.
[68] L. Y. Zanette, A. F. White, M. C. Allen, and M. Clinchy, *Perceived predation risk reduces the number of offspring songbirds produce per year*, Science, 334 (2011), pp. 1398–1401, https://doi.org/10.1126/science.1210908.
[69] C. Zhang, M. Jansen, L. De Meester, and R. Stoks, *Energy storage and fecundity explain deviations from ecological stoichiometry predictions under global warming and size-selective predation*, J. Anim. Ecol., 85 (2016), pp. 1431–1441.